Available online at www.sciencedirect.com
SCIENCE DIRECT®
Physica A 365 (2006) 282–288
PHYSICA A
www.elsevier.com/locate/physa

Wavelet entropy and fractional Brownian motion time series

D.G. Pérez[a,*], L. Zunino[b], M. Garavaglia[b,c], O.A. Rosso[d]

[a]Instituto de Física, Pontificia Universidad Católica de Valparaíso (PUCV), 23-40025 Valparaíso, Chile
[b]Centro de Investigaciones Ópticas (CIOp), CC. 124 Correo Central, 1900 La Plata, Argentina
[c]Departamento de Física, Facultad de Ciencias Exactas, Universidad Nacional de La Plata (UNLP), 1900 La Plata, Argentina
[d]Instituto de Cálculo, Facultad de Ciencias Exactas y Naturales, Universidad de Buenos Aires (UBA), Pabellón II, Ciudad Universitaria, 1428 Ciudad de Buenos Aires, Argentina

Received 18 January 2005; received in revised form 3 August 2005
Available online 24 October 2005

Abstract

We study the functional link between the Hurst parameter and the normalized total wavelet entropy when analyzing fractional Brownian motion (fBm) time series—these series are synthetically generated. Both quantifiers are mainly used to identify fractional Brownian motion processes [L. Zunino, D.G. Pérez, M. Garavaglia, O.A. Rosso, Characterization of laser propagation through turbulent media by quantifiers based on the wavelet transform, Fractals 12(2) (2004) 223–233]. The aim of this work is to understand the differences in the information obtained from them, if any.

Keywords: Fractional Brownian motion; Wavelet theory; Hurst parameter; Mean normalized total wavelet entropy

1. Introduction

When studying the laser beam propagation through a laboratory-generated turbulence [1] we have introduced two quantifiers: the *Hurst parameter*, H, and the *normalized total wavelet entropy* (NTWS), S_{WT}. The former quantifier was introduced to test how good the family of *fractional Brownian motion* [2] (fBm) processes models the wandering of such laser beam, while the NTWS is a more general quantifier aimed to study any given dynamic system [3]. Also, in a recent work we have analyzed the dynamic case: the laboratory-generated turbulence was set up to change in time [4]. We have observed that these quantifiers are correlated, but at the time only a qualitative argument was given. Furthermore, each one of these quantifiers have been used separately to obtain information from biospeckle phenomenon [5,6].

The fBm is the only one family of processes which is self-similar, with stationary increments, and Gaussian [7]. The normalized family of these Gaussian processes, B^H, is the one with $B^H(0) = 0$ almost surely, $\mathbb{E}[B^H(t)] = 0$, and covariance

$$\mathbb{E}[B^H(t)B^H(s)] = \tfrac{1}{2}(|t|^{2H} + |s|^{2H} - |t-s|^{2H}), \tag{1}$$

*Corresponding author. Fax: +56 32 273529.
E-mail addresses: dario.perez@ucv.cl (D.G. Pérez), lucianoz@ciop.unlp.edu.ar (L. Zunino), garavagliam@ciop.unlp.edu.ar (M. Garavaglia), oarosso@fibertel.com.ar (O.A. Rosso).

0378-4371/$ - see front matter © 2005 Elsevier B.V. All rights reserved.
doi:10.1016/j.physa.2005.09.060

for $s,t \in \mathbb{R}$. Here $\mathbb{E}[\cdot]$ refers to the average with Gaussian probability density. The power exponent H has a bounded range between 0 and 1. These processes exhibit memory, as can be observed from Eq. (1), for any Hurst parameter but $H = \frac{1}{2}$. In this case successive Brownian motion increments are as likely to have the same sign as the opposite, and thus there is no correlation. Otherwise, it is the Brownian motion that splits the family of fBm processes in two. When $H > \frac{1}{2}$ the correlations of successive increments decay hyperbolically, and their sum diverges, this sub-family of processes have long-memory. Besides, consecutive increments tend to have the same sign, these processes are *persistent*. For $H < \frac{1}{2}$, the correlations of the increments also decay hyperbolically but their sum is summable, and this sub-family presents short-memory. Since consecutive increments are more likely to have opposite signs, it is said that these are *anti-persistent*.

The wavelet analysis is one of the most useful tools when dealing with data samples. Thus, any signal can be decomposed by using a diadic discrete family $\{2^{j/2}\psi(2^j t - k)\}$—an *orthonormal* basis for $L^2(\mathbb{R})$—of translations and scaling functions based on a function ψ: the mother wavelet. This wavelet expansion has associated wavelet coefficients given by $C_j(k) = \langle \mathscr{S}, 2^{j/2}\psi(2^j \cdot - k)\rangle$. Each resolution level j has an associated energy $\mathscr{E}_j = \sum_k |C_j(k)|^2$. The *relative wavelet energy*, RWE, is

$$p_j = \frac{\mathscr{E}_j}{\mathscr{E}_{\text{tot}}}, \tag{2}$$

with $j \in \{-N, \ldots, -1\}$, where $N = \log_2 M$ with M the number of sample points, and $\mathscr{E}_{\text{tot}} = \sum_{j=-N}^{-1} \mathscr{E}_j$ is the total energy. Thus the NTWS is defined as (see Ref. [1] and references therein)

$$S_{\text{WT}} = -\sum_{j=-N}^{-1} p_j \cdot \log_2 p_j / S^{\max} \quad \text{with} \quad S^{\max} = \log_2 N. \tag{3}$$

For a signal originated from a fBm the energy per resolution level j and sampled time k can be calculated using the formalism introduced in Ref. [8], see Appendix,

$$\mathbb{E}|C_j(k)|^2 = 2\Gamma(2H+1)\sin(\pi H)2^{-j(2H+1)} \int_0^\infty \frac{|\hat{\psi}|^2(v)}{v^{2H+1}}, \tag{4}$$

for any mother wavelet election satisfying $\int_{\mathbb{R}} \psi = 0$. As you can observe the latter expression is independent of k. That is true for all stochastic processes with stationary increments [9,10]. On the other hand, a similar power-law behavior, $\mathbb{E}|C_j(k)|^2 \propto 2^{-j\alpha}$, is verified for stationary process displaying long-range dependence (LRD).[1] So, our results can also be applied for fractional Gaussian noises (fGn), for example.

From (4) the RWE for a finite data sample is

$$p_j = 2^{(j+1)(1+2H)} \frac{1 - 2^{-(1+2H)}}{1 - 2^{-N(1+2H)}}. \tag{5}$$

Observe that these coefficients are independent on wavelet basis. It can be easily computed from definition (2) and Eq. (4)—see again Appendix. And so it does the NTWS,

$$S_{\text{WT}}(N,H) = \frac{1}{\log_2 N}(1+2H)\left[\frac{1}{2^{1+2H}-1} - \frac{N}{2^{N(1+2H)}-1}\right] - \frac{1}{\log_2 N}\log_2\left[\frac{1-2^{-(1+2H)}}{1-2^{-N(1+2H)}}\right]. \tag{6}$$

As it was expected the entropy decreases when H increases, with H measuring the level of order of the signal.

2. Simulations and tests

To test the functional relation between the Hurst exponent and NTWS we have simulated 50 fBm data samples [11] for each $H \in \{0.1, 0.2, 0.3, 0.4, 0.5, 0.6, 0.7, 0.8, 0.9\}$. Since we have examined data of 5000 points in length in Ref. [1], these samples are set to the same length. For each set we estimate H and S_{WT}. Moreover, we

[1] Remember that $\alpha = 2H + 1$ for self-similar processes with stationary increments and $\alpha = 2H - 1$ for long-range dependent processes.

employ an orthogonal cubic spline function as mother wavelet. Among several alternatives, the cubic spline function is symmetric and combine in a suitable proportion smoothness with numerical advantages. It has become a recommendable tool for representing natural signals [12,13].

The Hurst parameter is estimated as usual (see Ref. [14] and references therein): by plotting the logarithm of the estimated energy per resolution level j and sampled time k,

$$\widehat{\mathscr{E}}_j(k) = \frac{1}{N_j} \sum_{k=1}^{N_j} |C_j(k)|^2, \tag{7}$$

versus j and fitting a minimum square line. The slope of the line is the desired estimator, $\widehat{H}$. In the above expression, $N_j = 2^j M$ is the number of coefficients at resolution level j.

For NTWS we start dividing the signal into N_T non-overlapping temporal windows with length L, $N_T = M/L$. The wavelet energy estimator at resolution level j for the time window i is given by

$$\widehat{\mathscr{E}}_j^{(i)} = \frac{1}{N_j^{(i)}} \sum_{k=(i-1)\cdot L+1}^{i\cdot L} |C_j(k)|^2 \quad \text{with } i = 1, \ldots, N_T, \tag{8}$$

where $N_j^{(i)}$ represents the number of wavelet coefficients at resolution level j corresponding to the time window i; while the total energy estimator in this time window will be $\widehat{\mathscr{E}}_{\text{tot}}^{(i)} = \sum_{j<0} \widehat{\mathscr{E}}_j^{(i)}$. The mean wavelet energy per resolution level j is considered instead of the total wavelet energy because we are interested in the low-frequency bands [3,14].

Hence, the time evolution estimators of RWE and NTWS will be given by

$$\widehat{p}_j^{(i)} = \widehat{\mathscr{E}}_j^{(i)} / \widehat{\mathscr{E}}_{\text{tot}}^{(i)}, \tag{9}$$

$$\widehat{S}_{\text{WT}}(i) = -\sum_{j<0} \widehat{p}_j^{(i)} \cdot \log_2 \widehat{p}_j^{(i)} / S^{\max}. \tag{10}$$

In order to obtain a quantifier for the whole time period under analysis [3] the temporal average is evaluated. The temporal average of NTWS is given by

$$\langle S_{\text{WT}} \rangle = \frac{1}{N_T} \sum_{i=1}^{N_T} \widehat{S}_{\text{WT}}^{(i)}, \tag{11}$$

and for the wavelet energy at resolution level j

$$\langle \mathscr{E}_j \rangle = \frac{1}{N_T} \sum_{i=1}^{N_T} \widehat{\mathscr{E}}_j^{(i)}; \tag{12}$$

then the total wavelet energy temporal average is defined as $\langle \mathscr{E}_{\text{tot}} \rangle = \sum_{j<0} \langle \mathscr{E}_j \rangle$. In consequence, a mean probability distribution $\{q_j\}$ representative for the whole time interval (the complete signal) can be defined as

$$q_j = \langle \mathscr{E}_j \rangle / \langle \mathscr{E}_{\text{tot}} \rangle, \tag{13}$$

with $\sum_j q_j = 1$ and the corresponding mean NTWS as

$$\widetilde{S}_{\text{WT}} = -\sum_{j<0} q_j \cdot \log_2 q_j / S^{\max}. \tag{14}$$

In Fig. 1 we compare H against its estimator. It has a good performance for $0.3 < H < 0.9$ and fails outside. Furthermore, the estimators fits better the larger values. Fig. 2 represents the temporal average of NTWS, $\langle S_{\text{WT}} \rangle$, and the mean NTWS, $\widetilde{S}_{\text{WT}}$, estimated with our procedure and compared against the theoretical result in Eq. (6) with $N = 12$. In our tests we worked in the range $j = -9, \ldots, -1$. As usual, boxplots [15] show lower and upper lines at the lower quartile (25th percentile of the sample) and upper quartile (75th percentile of the sample) and the line in the middle of the box is the sample median. The whiskers are lines extending from each end of the box indicating the extent of the rest of the sample. Outliers are marked by plus signs. These points may be considered the result of a data entry error or a poor measurement.

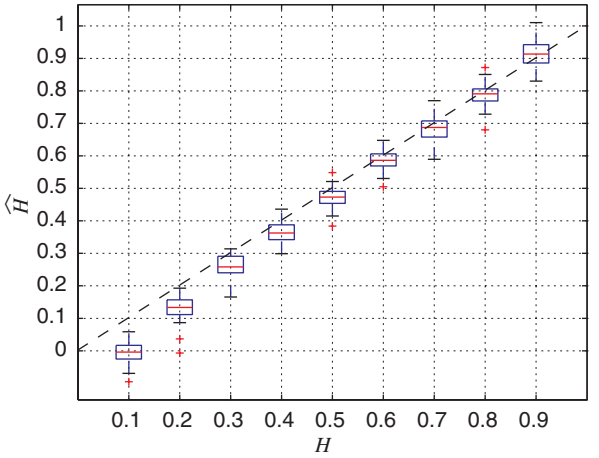

Fig. 1. The estimator for the Hurst parameter is plotted against the expected value, the dashed line is the identity.

3. Conclusions

For a fBm we have found, Eq. (6), there is an inverse dependence: as H grows the temporal average, $\langle S_{\mathrm{WT}}\rangle$, and mean NTWS, $\widetilde{S}_{\mathrm{WT}}$, diminishes. It is verified with the synthetic fBm data samples. This relation is logical, the spectrum has less high-frequency components as H gets higher and all the energy is closer to the origin, and, if H gets lower the energy contribution at high frequencies becomes relevant. Observe that the closer $\widehat{H}$ is to the exact value, the better are the results for both estimators of the entropy.

From Eq. (6) NTWS is a decreasing function of H. So, H is also a measure of the order of a signal. As far as we know this is a new interpretation of the information given by the Hurst parameter. In particular, the NTWS also contains information about the extension of the data set. Nevertheless, from a computational point of view the latter is independent on the scaling region because it is unnecessary the selection of one. On the other hand the logarithm in the entropy definition introduces important errors, as we see in Fig. 2. To narrow these it is necessary to increase the data samples. It should be stressed that extending the length of the data samples reduces the statistical error.

As a final remark, the NTWS should not be taken as a replacement for H when estimating the fBm characteristics of a signal. The former estimator allows to link these fractal stochastic processes with the generally used entropy concept.

Acknowledgements

This work was partially supported by Consejo Nacional de Investigaciones Científicas y Técnicas (CONICET, Argentina) and Pontificia Universidad Católica de Valparaíso (Project no. 123.774/2004, PUCV, Chile).

Appendix

Let us take as the signal $\mathscr{S}(t) = B^H(t,\omega)$, ω is fixed and represents one element of the statistic ensemble and it will be omitted hereafter. The wavelet coefficients are calculated using the orthonormal wavelet basis $\{2^{-j/2}\psi(2^{-j}\cdot - k)\}_{j,k\in\mathbb{Z}}$,

$$C_j^H(k) = \int_{\mathbb{R}} 2^{-j/2}\psi(2^{-j}s - k)B^H(s)\,\mathrm{d}s = 2^{(1/2+H)j}\int_{\mathbb{R}} \psi(s)B^H(s+k)\,\mathrm{d}s, \tag{15}$$

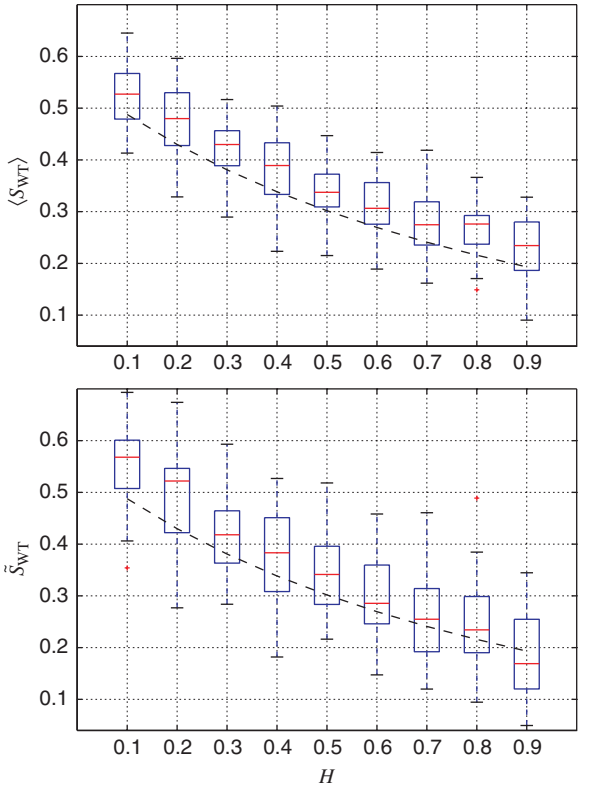

Fig. 2. $\langle S_{WT} \rangle$ (top) and $\tilde{S}_{WT}$ (bottom) are compared against $S_{WT}(12, H)$ (dashed line) as defined through Eq. (6).

for the last step we used the self-similar property of the fBm; that is, $B^H(t) \stackrel{d}{=} c^H B^H(c^{-1}t)$. Since the fBm can be written, using the chaos expansion described in Ref. [8], as

$$B^H(t) = \sum_{n=1}^{\infty} \langle M_H \mathbb{1}_{[0,t]}, \xi_n \rangle \mathscr{H}_{\varepsilon_n}(\omega),$$

where $\{\xi_n\}_{n\in\mathbb{N}}$ are the Hermite functions, and the operator M_H is defined as follows [16]:

$$\widehat{M_H \phi}(v) = c_H |v|^{1/2-H} \widehat{\phi}(v), \tag{16}$$

where the hat stands for the Fourier transform, $c_H^2 = \Gamma(2H+1)\sin(\pi H)$, and ϕ is any function in $L^2(\mathbb{R})$. Then, we introduce the following coefficients:

$$d_n^H(k) = \int_{\mathbb{R}} \langle M_H \mathbb{1}_{[0,s+k]}, \xi_n \rangle \psi(s)\, \mathrm{d}s, \tag{17}$$

to finally obtain

$$C_j^H(k) = 2^{(1/2+H)j} \sum_{n=1}^{\infty} d_n^H(k) \mathscr{H}_{\varepsilon_n}(\omega). \tag{18}$$

The evaluation of the coefficients $d_n^H(k)$ is straightforward from their definition and Eq. (16):

$$d_n^H(k) = -\frac{c_H}{\mathrm{i}^n} \int_{\mathbb{R}} \operatorname{sgn} v |v|^{-(1/2+H)} \Psi(v) \xi_n(v) \mathrm{e}^{-\mathrm{i}kv}\, \mathrm{d}v, \tag{19}$$

where $\Psi(v) = \widehat{\psi}(v)$.

The chaos expansion in Eq. (18) corresponds to a Gaussian process, then for integers j,k,j',k' the correlation is equal to [17]

$$\mathbb{E}[C_j^H(k)C_{j'}^{H*}(k')] = \sum_{n=1}^{\infty} 2^{(1/2+H)(j+j')} d_n^H(k) d_n^H(k').$$

Now, from Eq. (19) and orthogonality of the Hermite functions the above equation is rewritten in the following way:

$$\mathbb{E}[C_j^H(k)C_{j'}^{H*}(k')] = c_H^2 2^{(1/2+H)(j+j')} \int_{\mathbb{R}} |v|^{-(1+2H)} |\Psi(v)|^2 \mathrm{e}^{-\mathrm{i}(k-k')v}\,\mathrm{d}v, \tag{20}$$

which is the usual expression found in many works, see Ref. [9] and references therein. The integral has convergence problems near the origin. These are resolved choosing a mother wavelet ϕ with K null moments. That is,

$$\int_{\mathbb{R}} t^k \phi(t)\,\mathrm{d}t = 0,$$

for $k = 0,\ldots,K-1$. Therefore, $|\Psi(v)|^2 = a_1|v|^{2K} + a_2|v|^{2K+1} + o(|v|^{2K+1})$. When k and k' are far apart, i.e., $m = k - k' \to \infty$, the integral in Eq. (20) is dominated by the contribution of frequencies in the interval [0, 1], thus giving

$$\begin{aligned}\mathbb{E}[C_j^H(k)C_{j'}^{H*}(k')] &\approx 2a_1 c_H^2 2^{(1/2+H)(j+j')} \int_0^1 v^{2K-2H-1}\cos(mv)\,\mathrm{d}v \\ &= 2a_1 c_H^2 2^{(1/2+H)(j+j')} \Gamma(2K-2H)\cos(\pi(K-H))m^{2K-2H} + \mathcal{O}(m^{2K-2H-1}),\end{aligned} \tag{21}$$

for $K > H$. The coefficients of a wavelet expansion are highly correlated. But, for $j = j'$ and $k = k'$,

$$\begin{aligned}\mathbb{E}|C_j^H(k)|^2 &= c_H^2 2^{(1+2H)j} \int_{\mathbb{R}} |v|^{-(1+2H)} |\Psi(v)|^2\,\mathrm{d}v \\ &= 2\Gamma(2H+1)\sin(\pi H) 2^{(1+2H)j} \int_0^{\infty} v^{-(1+2H)} |\Psi(v)|^2\,\mathrm{d}v,\end{aligned} \tag{22}$$

we recover the mean energy by resolution level j and sampled time k. Therefore, the RWE is obtained replacing the above into Eq. (9):

$$p_j = \frac{2^{j(1+2H)}}{\sum_{j=-N}^{-1} 2^{j(1+2H)}} = \left[\frac{1-2^{-(1+2H)}}{1-2^{-N(1+2H)}}\right] 2^{(j+1)(1+2H)}, \tag{23}$$

where the last equation comes from the evaluation of the geometric series corresponding to the total energy. Its logarithm (base 2) is simply $\log_2 p_j = (1+2H)(j+1) + \log_2[1-2^{-(1+2H)}/1-2^{-N(1+2H)}]$. Finally, using these results in the definition of NTWS, it is

$$\begin{aligned}S_{\mathrm{WT}}(N,H) = &-\frac{1}{\log_2 N}\left[\frac{1-2^{-(1+2H)}}{1-2^{-N(1+2H)}}\right](1+2H)\sum_{j=-N}^{-1}(j+1)2^{(j+1)(1+2H)} \\ &-\frac{1}{\log_2 N}\left[\frac{1-2^{-(1+2H)}}{1-2^{-N(1+2H)}}\right]\log_2\left[\frac{1-2^{-(1+2H)}}{1-2^{-N(1+2H)}}\right]\sum_{j=-N}^{-1}2^{(j+1)(1+2H)},\end{aligned} \tag{24}$$

then handling the geometric sums carefully we obtain Eq. (6).

References

[1] L. Zunino, D.G. Pérez, M. Garavaglia, O.A. Rosso, Characterization of laser propagation through turbulent media by quantifiers based on the wavelet transform, Fractals 12 (2) (2004) 223–233.

[2] B.B. Mandelbrot, J.W. Van Ness, Fractional Brownian motions, fractional noises and applications, SIAM Rev. 4 (1968) 422–437.

[3] O.A. Rosso, S. Blanco, J. Yordanova, V. Kolev, A. Figliola, M. Schürmann, E. Başar, Wavelet entropy: a new tool for analysis of short duration brain electrical signals, J. Neurosci. Method 105 (2001) 65–75.
[4] L. Zunino, D.G. Pérez, M. Garavaglia, O.A. Rosso, Characterization of laser propagation through turbulent media by quantifiers based on the wavelet transform: dynamic study, Physica A (2005), in press.
[5] I. Passoni, H. Rabal, C.M. Arizmendi, Characterizing dynamic speckle time series with the Hurst coefficient concept, Fractals 12 (3) (2004) 319–329.
[6] I. Passoni, A. Dai Pra, H. Rabal, M. Trivi, R. Arizaga, Dynamic speckle processing using wavelets based entropy, Opt. Commun. 246 (1–3) (2005) 219–228.
[7] G. Samorodnitsky, M.S. Taqqu, Stable non-Gaussian random processes, Stochastic Modeling, Chapman & Hall, London, UK, 1994.
[8] D.G. Pérez, L. Zunino, M. Garavaglia, Modeling the turbulent wave-front phase as a fractional Brownian motion: a new approach, J. Opt. Soc. Am. A 21 (10) (2004) 1962–1969.
[9] P. Flandrin, Wavelet analysis and synthesis of fractional Brownian motion, IEEE Trans. Inf. Theory IT-38 (2) (1992) 910–917.
[10] E. Masry, The wavelet transform of stochastic processes with stationary increments and its applications to fractional Brownian motion, IEEE Trans. Inf. Theory IT-39 (1) (1993) 260–264.
[11] J.-F. Coeurjolly, Statistical inference for fractional and multifractional Brownian motions, Ph.D. Thesis, Laboratoire de Modélisation et Calcul - Institut d'Informatique el Mathématiques Appliquées de Grenoble, 2000. URL <http://bibliotheque.imag.fr/publications/theses/2000>.
[12] M. Unser, Spline: a perfect fit for signal and image processing, IEEE Signal Process. Mag. 16 (1999) 22–38.
[13] P. Thévenaz, T. Blu, M. Unser, Interpolation revisited, IEEE Trans. Med. Imaging 19 (7) (2000) 739–758.
[14] P. Abry, P. Flandrin, M.S. Taqqu, D. Veitch, Wavelets for the analysis estimation and synthesis of scaling data, in: K. Park, W. Willinger (Eds.), Self-similar Network Traffic and Performance Evaluation, Wiley, New York, 2000.
[15] J.W. Tukey, Exploratory Data Analysis, Addison-Wesley, Reading, MA, 1977.
[16] R.J. Elliott, J. van der Hoek, A general fractional white noise theory and applications to finance, Math. Finance 13 (2003) 301–330.
[17] H. Holden, B. Øksendal, J. Ubøe, T. Zhang, Stochastic partial differential equations: a modeling, white noise functional approach, in: Probability and Its Applications, Birkhäuser, Basel, 1996.